

Theory of Threading Edge and Screw Dislocations in GaN

J. Elsner* and R. Jones

Department of Physics, University of Exeter, Exeter, EX4 4QL, United Kingdom

P. K. Sitch, V. D. Porezag, M. Elstner, and Th. Frauenheim

Technische Universität, Theoretische Physik III, D-09107 Chemnitz, Germany

M. I. Heggie

CPES, University of Sussex, Falmer, Brighton, BN1 9QJ, United Kingdom

S. Öberg

Department of Mathematics, University of Luleå, Luleå, S97 187, Sweden

P. R. Briddon

Department of Physics, University of Newcastle upon Tyne, Newcastle, NE1 7RU, United Kingdom

(Received 8 July 1997)

The atomic structures, electrical properties, and line energies for threading screw and threading edge dislocations of wurtzite GaN are calculated within the local-density approximation. Both dislocations are electrically inactive with a band gap free from deep levels. These results are understood to arise from relaxed core structures which are similar to $(10\bar{1}0)$ surfaces. [S0031-9007(97)04460-8]

PACS numbers: 61.72.Bb, 61.72.Lk

Device quality wurtzite-GaN (α) can be grown using metalorganic chemical vapor phase deposition (MOCVD) on (0001) sapphire substrates. The large lattice misfit results in dislocation tangles near the interface but isolated threading dislocations, parallel to \mathbf{c} , with densities $\sim 10^9 \text{ cm}^{-2}$ and Burgers vectors \mathbf{c} , \mathbf{a} , and $\mathbf{c} + \mathbf{a}$ persist beyond $\sim 0.5 \mu\text{m}$ above the interface [1–3] and thus cross the active region of the devices. An unexpected finding [4,5] is that these dislocations do not lead to a pronounced reduction in the device lifetime of the light-emitting diodes [6] or blue lasers [7]. Recent cathodoluminescence (CL) studies of the yellow luminescence (YL) centered at $\sim 2.2 \text{ eV}$ have shown that the YL is spatially nonuniform and can be correlated with extended defects and especially low angle grain boundaries which contain dislocations [8]. On the other hand, atomic force microscopy in combination with CL has led to the conclusion that threading dislocations act as nonradiative recombination centers and degrade the luminescence efficiency in the blue light spectrum of the epilayers [9].

Screw dislocations in α -GaN have elementary Burgers vector $\pm\mathbf{c}$ and are unusual in often being associated with nanopipes with diameters 50–250 Å [10]. Pure edge dislocations lying on $\{10\bar{1}0\}$ planes are a dominant species of dislocation in α -GaN grown by MOCVD on (0001) sapphire, occurring at extremely high densities of $\sim 10^8$ – 10^{11} cm^{-2} .

Here we explore the structure and electronic properties of threading screw and edge dislocations in GaN using an *ab initio* local-density functional (LDF) cluster method, AIMPRO, and a density functional based tight binding method DF-TB which can be used for both clusters

and supercells. The AIMPRO method [11,12] uses norm-conserving pseudopotentials [13] and a basis of s - and p -Gaussian orbitals for the pseudowave functions together with an ancillary basis to fit the charge density. In the current application we use a large real-space basis set of 20 (16) Gaussian orbitals on every Ga (N) atom. Applied to a 72 atom H-terminated stoichiometric cluster arranged as in wurtzite, it gave GaN bond lengths within 4% of experiment and a maximum vibrational frequency of 729 cm^{-1} compared with 741 cm^{-1} experimentally found for the $E_1(\text{LO})$ mode [14].

The DF-TB method uses a basis of numerically derived s , p , and d confined atomic orbitals and all two-center integrals of the LDF Hamiltonian and overlap matrix are evaluated. Charge transfer is taken into account through the incorporation of a self-consistency (SC) scheme for the Mulliken charges based on a second order expansion of the Kohn-Sham ground state energy in terms of charge density fluctuations at a given proper input density. In this formalism the Mulliken charges for each atom are evaluated after each step of the SC cycle. The diagonal elements of the Hamilton matrix employed at the next iteration are then modified by charge dependent contributions in order to describe the change in the atomic potentials due to the charge transfer for that iteration. The off-diagonal entries have additional charge dependent terms coming from the Coulomb potential of the ions. They decay with $1/r$ and thus account for the Madelung energy of the system. For further details of the DF-TB method see Refs. [15,16]. As an illustrative benchmark of the DF-TB method, we choose quantitative calculations for the nonpolar GaN $(10\bar{1}0)$ surface, since very similar

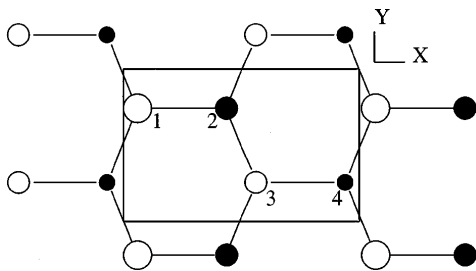


FIG. 1. Schematic top view of the $(10\bar{1}0)$ surface of wurtzite GaN. Atoms 1 and 2 form a dimer in the surface layer. Atoms 3 and 4 form the second layer.

configurations occur in the dislocation cores. Figure 1 and Table I give details of the calculated geometrical structure of the nonpolar GaN $(10\bar{1}0)$ surface along with the results of first-principles calculations by Northrup and Neugebauer [17]. The structures are very similar. Moreover, the calculated absolute surface energy of $121 \text{ meV}/\text{\AA}^2$ agrees very well with the $118 \text{ meV}/\text{\AA}^2$ given in [17].

We now apply these methods to dislocations in GaN. Isotropic elasticity theory was used to generate the initial positions of the atoms. Relaxations were then carried out using the conjugate gradient algorithm. In the AIM-PRO case dislocations were modeled in 392 atom stoichiometric clusters. In the DF-TB case the dislocations are modeled in large clusters and in 576 atom $(12 \times 12 \times 1)$ supercells containing a dislocation dipole in each cell in order to calculate the local line energy of the dislocations. In analogy to the formation energy for planar defects [18], we define the local line energy of extended defects as $E_{\text{line}} = \frac{1}{2L}(E - E_{\text{bulk}})$, where E is the total energy of a supercell containing two line defects, E_{bulk} is the total energy of a bulk system with the same number of atoms, and $L = 5.19 \text{ \AA}$ is the length of the supercell of the line defect in the (0001) direction.

We consider first the screw dislocation ($b = \pm[000c]$) with a full core. Both methods found heavily distorted bond lengths (see Table II) yielding deep gap states ranging from $0.9\text{--}1.6 \text{ eV}$ above the valence band maximum, VBM, and shallow gap states at $\sim 0.2 \text{ eV}$ below the conduction band minimum, CBM. An analysis of these gap states revealed that the states above the VBM are localized on N core atoms, whereas the states below CBM are localized on core atoms but have mixed Ga and N

TABLE I. Atomic displacements in \AA for the top two layers of atoms at the GaN $(10\bar{1}0)$ surface. Atom numbers refer to Fig. 1. Values in brackets are results of Ref. [17].

Atom	Δx	Δy	Δz
1 ($\text{Ga}_{3 \times \text{coord.}}$)	-0.10 (-0.11)	0.0	-0.23 (-0.20)
2 ($\text{N}_{3 \times \text{coord.}}$)	0.03 (0.01)	0.0	-0.01 (0.02)
3 ($\text{Ga}_{4 \times \text{coord.}}$)	0.01 (0.05)	0.0	0.08 (0.05)
4 ($\text{N}_{4 \times \text{coord.}}$)	0.04 (0.05)	0.0	0.07 (0.05)

TABLE II. Bond lengths, min-max (average), in \AA and bond angles (min-max) in degrees for the most distorted atoms at the core center of the full-core screw dislocation ($b = [0001]$).

Atom	Bond lengths	Bond angles
1 ($\text{Ga}_{4 \times \text{coord.}}$)	1.85–2.28 (2.14)	68–137
2 ($\text{N}_{4 \times \text{coord.}}$)	1.89–2.28 (2.13)	71–136

character. A calculation in a supercell containing a screw dipole consisting of two dislocations with $b = [000c]$ and $-[000c]$, which are symmetrically equivalent, confirmed these results and gave a high line energy of $4.88 \text{ eV}/\text{\AA}$. This is mainly the core energy of each screw dislocation along with the elastic energy stored in a cylinder of diameter roughly equal to the distance between the cores, 19.1 \AA .

We now inquire whether this energy is reduced if material is removed from the core. Accordingly, a similar calculation was carried out using the same supercell, but with the hexagonal core of each screw removed leading to a pair of open-core dislocations with diameters $d \approx 7.2 \text{ \AA}$. The relaxed structure (Fig. 2) preserved the hexagonal core character, demonstrating that the internal surfaces of the dislocation cores shown in (Fig. 3) are similar to $(10\bar{1}0)$ facets except for the topological singularity required by a Burgers circuit. Comparing the distortions of the atoms situated at the wall of the open-core (Table III) with the corresponding atoms at the $(10\bar{1}0)$ surface (Table IV), we see that in both cases the threefold coordinated Ga (N) atoms adopt sp^2 (p^3) like hybridizations which lower the surface energy and clean the gap [17]. However, in contrast to the $(10\bar{1}0)$ surface, shallow gap states remain. Calculations were carried out for a distorted $(10\bar{1}0)$ surface, i.e., a $(10\bar{1}0)$ surface in a unit cell where the unit cell vectors were modified to give a distorted surface corresponding to that of the wall of

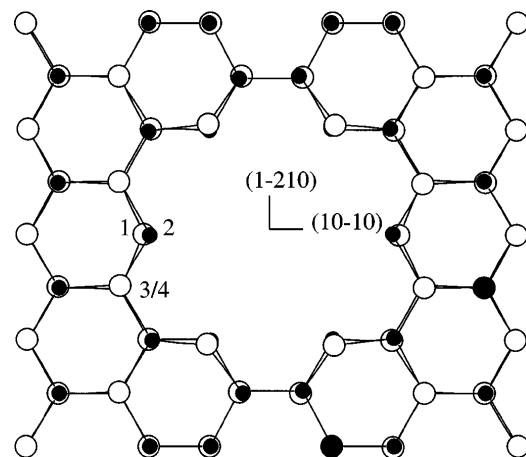


FIG. 2. Top view (in $[0001]$) of the relaxed core of the open-core screw dislocation ($b = [0001]$). The threefold coordinated atoms 1 (Ga) and 2 (N) adopt a hybridization similar to the $(10\bar{1}0)$ surface atoms.

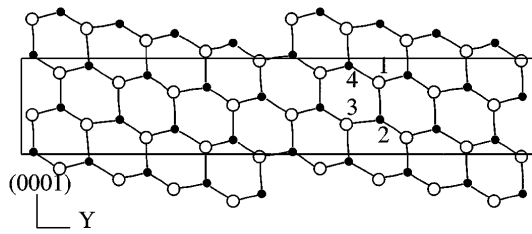


FIG. 3. Projection of the wall of the open-core ($d = 7.2 \text{ \AA}$) screw dislocation ($b = [0001]$). The threefold coordinated atoms 1 (Ga) and 2 (N) adopt a hybridization similar to the $(10\bar{1}0)$ surface atoms.

the open-core screw dislocation with diameter $d = 7.2 \text{ \AA}$. We find that the distorted $(10\bar{1}0)$ surface has a spectrum with shallow states very similar to those of the open-core screw dislocation with $d = 7.2 \text{ \AA}$. We also calculated the spectrum for a nanopipe with $d = 7.2 \text{ \AA}$ but without a dislocation core. This, like the undistorted $(10\bar{1}0)$ surface, possesses no gap states at all. These results indicate that the shallow states in the open-core screw dislocation with diameter $d = 7.2 \text{ \AA}$ can be attributed to the distortion arising from the dislocation Burgers vector. Calculations for a series of different distortions of the $(10\bar{1}0)$ surface also suggest that open-core screw dislocations with a diameter $d \geq 20 \text{ \AA}$ should have no gap states at all. As can be seen in Table III the distortion in the open-core screw dislocation is significantly less than that in the full-core screw dislocation (see Table II). It is therefore not surprising that the calculated line energy of 4.55 eV/\AA is lower than the line energy of the full-core screw dislocation. The energy required to form the surface at the wall is more than compensated by the energy gained by reducing the strain. However, a further opening gave a higher line energy, and we conclude that the equilibrium diameter is 7.2 \AA . It is unlikely that isotropic elasticity theory can describe the severely distorted full-core dislocation which limits the usefulness of Frank's expression relating to the diameter of an open-core dislocation [19]. Dislocations with large open diameters that are observed might arise from kinetic factors relating to the coalescence of misaligned interfacial growth islands [2,20] leading to pinholes which do not grow out [21].

In the same way threading edge dislocations were modeled by relaxation of a cluster containing one dislocation with Burgers vector $a[11\bar{2}0]/3$ and a supercell with a dis-

TABLE III. Bond lengths, min-max (average) in \AA and bond angles, min-max (average) in degrees for the most distorted atoms at the wall of the open-core screw dislocation ($b = [0001]$). Atom numbers refer to Figs. 2 and 3.

Atom	Bond lengths	Bond angles
1 ($\text{Ga}_{3 \times \text{coord.}}$)	1.86–1.89 (1.88)	107–123 (117)
2 ($\text{N}_{3 \times \text{coord.}}$)	1.88–2.05 (1.96)	102–111 (108)
3 ($\text{Ga}_{4 \times \text{coord.}}$)	1.89–2.07 (1.96)	100–122
4 ($\text{N}_{4 \times \text{coord.}}$)	1.93–2.03 (1.97)	98–120

TABLE IV. Bond lengths, min-max (average) in \AA and bond angles, min-max (average) in degrees for the top two layers of atoms at the $\text{GaN}(10\bar{1}0)$ surface. Atom numbers refer to Fig. 1.

Atom	Bond lengths	Bond angles
1 ($\text{Ga}_{3 \times \text{coord.}}$)	1.83–1.88 (1.86)	116–117 (117)
2 ($\text{N}_{3 \times \text{coord.}}$)	1.83–1.92 (1.89)	107–111 (108)
3 ($\text{Ga}_{4 \times \text{coord.}}$)	1.91–2.02 (1.94)	107–112
4 ($\text{N}_{4 \times \text{coord.}}$)	1.88–2.03 (1.93)	99–115

location dipole. The relaxed core is shown in Fig. 4. The corresponding bond lengths and bond angles of the most distorted atoms are given in Table V. Again the threefold coordinated Ga (N) atoms (Nos. 1 and 2 in Fig. 4) relax towards sp^2 (p^3) leading to empty Ga lone pairs pushed towards the CBM, and filled lone pairs on N atoms lying near the VBM, in a manner identical to the $(10\bar{1}0)$ surface. Thus threading edge dislocations are also electrically inactive.

From a supercell calculation, we obtain a line energy of 2.19 eV/\AA for the threading edge dislocation which is considerably lower than that found for the empty screw dislocation. This can be interpreted by noting that the edge dislocation has a smaller number of threefold coordinated atoms than the open-core screw dislocation as well as a smaller elastic strain energy arising from the smaller Burgers vector. This last energy is proportional to kb^2 . Here, b is the magnitude of the Burgers vector, and the constant k is equal to 1 for the screw dislocation and $\frac{1}{1-\nu}$ for the edge dislocations, where ν is Poisson's ratio (0.37 for GaN [22]). Thus the ratio of the elastic energies is $E_{\text{screw}}/E_{\text{edge}}$ which is approximately 1.66. Our calculation gives the ratio of the line energies, which includes the core energies, to be 2.08.

In analogy to the open-core screw dislocations we have investigated whether the energy of the threading edge dislocation could be lowered by removing the most distorted core atoms (see Fig. 4). However, removal of either the lines of atoms 9 and 10 or the atoms 1, 2, 3, 4, 5, 6, 7, 8, and their equivalents on the right leads to higher line energies. This implies that, in contrast with screw

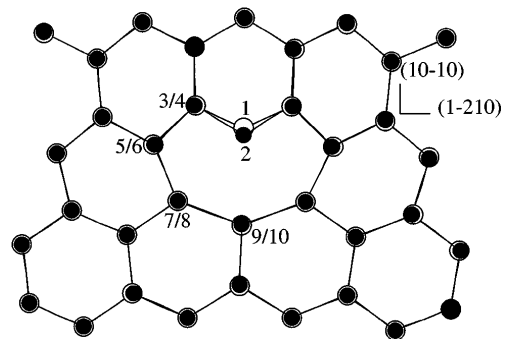


FIG. 4. Top view (in $[0001]$) of the relaxed core of the threading edge dislocation ($b = [11\bar{2}0]$). The threefold coordinated atoms 1 (Ga) and 2 (N) adopt a hybridization similar to the $(10\bar{1}0)$ surface atoms.

TABLE V. Bond lengths, min-max (average) in Å and bond angles, min-max (average) in degrees for the most distorted atoms at the core of the threading edge dislocation ($b = \frac{1}{3}[11\bar{2}0]$). Atom numbers refer to Fig. 4.

Atom	Bond lengths	Bond angles
1 (Ga _{3×coord.})	1.85–1.86 (1.85)	112–118 (116)
2 (N _{3×coord.})	1.88–1.89 (1.86)	106–107 (106)
3 (Ga/N _{4×coord.})	1.86–1.95 (1.91)	97–119
4 (Ga/N _{4×coord.})	1.92–2.04 (1.97)	100–129
5 (Ga/N _{4×coord.})	2.01–2.21 (2.06)	94–125
6 (Ga/N _{4×coord.})	2.00–2.21 (2.11)	100–122

dislocations, the threading edge dislocations should exist with a full core. It is worth noting, however, that the core atoms 9 and 10 have very stretched bonds with bond lengths ranging from 2.0 to 2.2 Å and thus give rise to a stress field which could act as a trap for intrinsic defects and impurities, e.g., the Ga vacancy O complex which could be responsible for the YL in *n*-type GaN [23]. Results on defect complexes in the stress field of dislocations is under current investigation and will be published in a forthcoming paper.

In conclusion, the density functional calculations reveal that the common threading screw and threading edge dislocations in wurtzite GaN are electrically inactive. A comparison of the calculated line energies explains why the screw dislocations exist as open-core dislocations, whereas the threading edge dislocations have filled cores. It seems that the stress fields are sufficiently large that impurities might well be trapped.

We gratefully acknowledge Deutsche Forschungsgemeinschaft, NFR, TFR, and PDC at KTH in Sweden for financial support and computer time on the SP2. We thank the HPCI committee of the EPSRC for computer time on the T3D (Grant Reference GR/K42301) and David Cherns for helpful discussions.

*On leave from Technische Universität Chemnitz.

[1] X. H. Wu, L. M. Brown, D. Kopolnek, S. Keller, B. Keller, S. P. DenBaars, and S. J. Speck, *J. Appl. Phys.* **80**, 3228 (1996).

[2] X. J. Ning, F. R. Chien, and P. Pirouz, *J. Mater. Res.* **11**, 580 (1996).

[3] F. A. Ponce, D. Cherns, W. T. Young, and J. W. Steeds, *Appl. Phys. Lett.* **69**, 770 (1996).

[4] S. D. Lester, F. A. Ponce, M. G. Cranford, and D. A. Steigerwald, *Appl. Phys. Lett.* **66**, 1249 (1996).

[5] L. Sugiura, *J. Appl. Phys.* **81**, 1633 (1997).

[6] S. Nakamura, T. Mukai, and M. Senoh, *J. Appl. Phys.* **76**, 8189 (1994).

[7] S. Nakamura, M. Senoh, S. Nagahama, N. Iwasa, T. Yamada, T. Matsushita, H. Kiyohu, and Y. Sguimoto, *Jpn. J. Appl. Phys.* **35**, L74 (1996).

[8] F. A. Ponce, D. B. Bour, W. Gotz, and P. J. Wright, *Appl. Phys. Lett.* **68**, 57 (1996). Recent combined cathodoluminescence and atomic force microscopy points to threading dislocations as a source for these centers [9].

[9] S. J. Rosner, E. C. Carr, M. J. Ludowise, G. Giralami, and H. I. Erikson, *Appl. Phys. Lett.* **70**, 420 (1997).

[10] W. Qian, M. Skowronski, K. Doverspike, L. B. Rowland, and D. K. Gaskill, *J. Cryst. Growth* **151**, 396 (1995).

[11] R. Jones, *Philos. Trans. R. Soc. London A* **350**, 189 (1995).

[12] R. Jones and P. R. Briddon, in *The ab initio Cluster Method and the Dynamics of Defects in Semiconductors, Semiconductors and Semimetals: Identification of Defects in Semiconductors*, edited by M. Stavola (Academic Press, New York, 1997).

[13] G. B. Bachelet, D. R. Hamann, and M. Schlüter, *Phys. Rev. B* **26**, 4199 (1982).

[14] D. Behr, J. Wagner, J. Schneider, H. Amano, and I. Akasaki, *Appl. Phys. Lett.* **68**, 2404 (1996).

[15] D. Porezag, Th. Frauenheim, and Th. Köhler, *Phys. Rev. B* **51**, 12 947 (1995).

[16] M. Elstner, D. Porezag, G. Jungnickel, Th. Frauenheim, and G. Seiffert, *Phys. Rev. Lett.* (to be published).

[17] J. E. Northrup and J. Neugebauer, *Phys. Rev. B* **53**, 10 477 (1996).

[18] J. E. Northrup, J. Neugebauer, and L. T. Romano, *Phys. Rev. Lett.* **77**, 103 (1996).

[19] F. C. Frank, *Acta Crystallogr.* **4**, 497 (1951).

[20] D. Cherns, W. T. Young, J. W. Steeds, F. A. Ponce, and S. Nakamura, *J. Cryst. Growth* (to be published).

[21] Z. Liliental-Weber *et al.*, in *The Proceedings of ICDS 19* (to be published).

[22] V. A. Savastenko and A. U. Shelog, *Phys. Status Solidi A* **48**, K135 (1978).

[23] J. Neugebauer and C. Van de Walle, *Appl. Phys. Lett.* **69**, 503 (1996).